Uludağ Üniversitesi Tıp Fakültesi Dergisi
Journal of Uludağ University Medical Faculty
52, 1885572, 2026
DOI: https://doi.org/10.32708/uutfd.1885572

ORIGINAL RESEARCH

Breast Magnetic Resonance Imaging as a Problem-Solving Tool in Patients with Mammographic Architectural Distortion

Seçil GÜNDOĞDU[1], Leman GÜNBEY KARABEKMEZ[2]

[1] Department of Radiology, Ankara Bilkent City Hospital, Ankara, Türkiye.
[2] Department of Radiology, Ankara Yildirim Beyazit University, Ankara, Türkiye.

ABSTRACT

Architectural distortion detected on full-field digital mammography represents a significant diagnostic challenge due to its association with both benign and malignant pathologies. This retrospective study evaluated the diagnostic performance of breast magnetic resonance imaging (MRI) in differentiating benign and malignant lesions in patients with mammographic architectural distortion. Sixty-two patients (age range, 27–78 years; median, 48 years) examined between January 2020 and March 2021 were included. Histopathological confirmation was available for 36 lesions, while 26 benign lesions were validated by at least two years of imaging follow-up. MRI features analyzed included lesion type, margin characteristics, internal enhancement pattern, background parenchymal enhancement, T2 signal intensity, diffusion restriction, apparent diffusion coefficient (ADC) values, and kinetic curve type. Of the evaluated lesions, 17 were malignant and 19 were benign. Malignancy was significantly associated with non-circumscribed margins, heterogeneous or rim enhancement, diffusion restriction, low ADC values, and wash-out kinetic patterns, whereas benign lesions were more frequently characterized by high T2 signal intensity and homogeneous enhancement (all $p < 0.05$). Minimal background parenchymal enhancement was more common in malignant cases, while marked enhancement was observed exclusively in benign lesions. MRI showed limited ability to reliably differentiate radial scars from invasive carcinoma. Overall, breast MRI provided additional diagnostic value in the evaluation of mammographic architectural distortion. A multiparametric approach integrating morphologic, functional, and dynamic MRI features improved diagnostic accuracy and may help reduce unnecessary biopsies, while highlighting key imaging predictors of malignancy.

Keywords: Architectural distortion. Diffusion-weighted imaging. Kinetic curve analysis. Apparent diffusion coefficient. Breast magnetic resonance imaging.

Mamografide Saptanan Yapısal Bozulmalarda Meme Manyetik Rezonans Görüntülemenin Tanısal Sorun Çözücü Rolü

ÖZET

Tam alan dijital mamografide saptanan yapısal bozulma, hem benign hem de malign patolojilerle ilişkili olabilmesi nedeniyle önemli bir tanısal güçlük oluşturmaktadır. Bu retrospektif çalışmada, mamografide yapısal bozulma saptanan hastalarda benign ve malign lezyonların ayırt edilmesinde meme manyetik rezonans görüntülemenin (MRG) tanısal performansı değerlendirilmiştir. Ocak 2020–Mart 2021 tarihleri arasında incelenen 62 hasta (yaş aralığı 27–78, medyan 48) çalışmaya dahil edilmiştir. Otuz altı lezyon histopatolojik olarak doğrulanmış, 26 benign lezyon ise en az iki yıllık görüntüleme takibi ile teyit edilmiştir. MRG'de lezyon tipi, kenar özellikleri, internal kontrastlanma paterni, arka plan parankimal kontrastlanma düzeyi, T2 sinyal intensitesi, difüzyon kısıtlılığı, görünür difüzyon katsayısı (ADC) değerleri ve kinetik eğri tipi değerlendirilmiştir. Değerlendirilen lezyonların 17'si malign, 19'u benign olarak saptanmıştır. Malignite; düzensiz kenar, heterojen veya rim tarzı kontrastlanma, difüzyon kısıtlılığı, düşük ADC değerleri ve wash-out kinetik patern ile anlamlı düzeyde ilişkili bulunurken, benign lezyonlar daha sıklıkla yüksek T2 sinyal intensitesi ve homojen kontrastlanma göstermiştir (tümü $p<0,05$). Minimal arka plan parankimal kontrastlanma malignite ile ilişkiliyken, belirgin kontrastlanma yalnızca benign olgularda izlenmiştir. Meme MRG, radial skar ile invaziv karsinom ayrımında sınırlı bir ayırt edici performans göstermiştir. Sonuç olarak, mamografide saptanan yapısal bozulmaların değerlendirilmesinde meme MRG ek tanısal katkı sağlamaktadır. Morfolojik, fonksiyonel ve dinamik özelliklerin birlikte değerlendirildiği multiparametrik yaklaşım tanısal doğruluğu artırabilir ve gereksiz biyopsilerin azaltılmasına katkıda bulunabilirken, malignite için önemli görüntüleme belirteçlerini de vurgulamaktadır.

Anahtar Kelimeler: Yapısal bozulma. Meme manyetik rezonans görüntüleme. Difüzyon ağırlıklı görüntüleme. Görünür difüzyon katsayısı. Kinetik eğri analizi.

Date Received: 9.February.2026
Date Accepted: 19.March.2026

Dr. Seçil GÜNDOĞDU
Department of Breast Radiology, Ankara Bilkent City Hospital
Ankara, Türkiye
E-mail: drsecilgundogdu@gmail.com

AUTHORS' ORCID INFORMATION
Seçil GÜNDOĞDU: 0000-0002-6254-3022
Leman GÜNBEY KARABEKMEZ: 0000-0001-9862-0192

Architectural distortion (AD) is defined by the American College of Radiology Breast Imaging Reporting and Data System (BI-RADS) as distortion of the normal breast parenchymal architecture without a definable mass, including spiculations radiating from a point or focal parenchymal retraction[1]. It represents one of the most challenging mammographic findings and is recognized as the third most common mammographic manifestation of nonpalpable breast cancer after masses and calcifications[2]. However, AD is not specific for malignancy and may also be associated with benign entities such as radial scar, sclerosing adenosis, fibrotic changes, or postsurgical alterations, leading to diagnostic uncertainty[3,4].

With the increasing adoption of digital breast tomosynthesis (DBT), detection rates of architectural distortion have improved; nevertheless, specificity remains limited, and false-positive findings are common[5]. Mammographic AD, particularly when categorized as BI-RADS 3 or 4, frequently prompts tissue sampling because of its association with malignancy[6,7]. Despite this approach, a substantial proportion of biopsied AD lesions ultimately prove to be benign, underscoring the need for adjunct imaging methods to refine risk stratification and reduce unnecessary biopsies.

Breast magnetic resonance imaging (MRI) is the most sensitive imaging modality for breast cancer detection and has an established role in staging, screening high-risk populations, and problem-solving in indeterminate mammographic findings[8]. In the setting of architectural distortion, MRI has been shown to provide a high negative predictive value (NPV); however, its clinical utility may be limited by relatively low specificity and false-positive enhancement patterns. The incorporation of functional techniques, particularly diffusion-weighted imaging (DWI) and apparent diffusion coefficient (ADC) analysis, has been shown to improve lesion characterization and diagnostic specificity when combined with morphologic and dynamic contrast-enhanced features[9,10].

Given these considerations, the present study aimed to evaluate the diagnostic contribution of combined morphologic and functional MRI features in differentiating benign and malignant lesions in patients with mammographic AD, with particular emphasis on improving diagnostic confidence and reducing unnecessary biopsies.

Materials and Methods

Ethics Approval

This study was performed in line with the principles of the Declaration of Helsinki. Approval was granted by the Ethics Committee of Ankara Bilkent Şehir Hospital (Date: 13/08/2025 No: TABED 1/1607/2025*)*. Given the retrospective design of this study and the strict measures taken to protect patient confidentiality, the requirement for informed consent was waived.

Subjects

Patients were retrospectively identified by screening the hospital radiology database for cases with mammographic AD who subsequently underwent breast MRI between January 2020 and March 2021. A total of 62 women aged between 18 and 76 years (mean age, 50.47±8.75 years) were included in the study.

Patients were eligible for inclusion if AD was identified on full-field digital mammography (FFDM) as the primary imaging finding, with or without associated nonspecific asymmetry, and without a definite mass lesion. Architectural distortion was confirmed independently by two experienced breast radiologists in accordance with the American College of Radiology BI-RADS criteria.

Cases with AD accompanied by suspicious pleomorphic or segmental microcalcifications were excluded to avoid confounding imaging features that independently mandate biopsy. In addition, patients with a history of prior breast biopsy, surgery, radiotherapy, chemotherapy, or neoadjuvant treatment in the same breast were excluded to eliminate post-interventional architectural changes that could mimic true AD. Examinations with insufficient image quality for reliable interpretation were also excluded.

Only lesions categorized as BI-RADS 3 or BI-RADS 4 on mammography were included in the analysis, as these categories represent the subgroup in which breast MRI may provide incremental diagnostic value and influence clinical management. Lesions classified as BI-RADS 5 were excluded due to their high pretest probability of malignancy and direct indication for biopsy.

All included patients underwent contrast-enhanced breast MRI within two months following FFDM. Diagnostic confirmation was obtained either by histopathological analysis from biopsy or surgical specimens, or by at least two years of clinical and imaging follow-up confirming benignity.

Accordingly, this study represents a real-world problem-solving MRI cohort aimed at refining biopsy decisions in patients with indeterminate mammographic AD.

FFDM examination

All FFDM examinations were performed using a Senographe Pristina system (GE Healthcare, Buc, France) with standard craniocaudal (CC) and mediolateral oblique(MLO). All images were viewed

on HP Z440 Workstation 8770000-25 REV 4 (GE Healthcare) equipped with MG-approved monitors (Barco NV, 5MP Mammo, Barco, Kortrijk, Belgium).

MRI technique

All breast MRI examinations were performed using a 3.0-T scanner (Signa Pioneer, General Electric Medical Systems, Milwaukee, WI, USA) with a dedicated 16-channel bilateral breast coil. Imaging was performed with patients in the prone position.

The MRI protocol included axial T1-weighted fast spin-echo sequences, axial and sagittal T2-weighted fat-suppressed sequences, diffusion-weighted imaging, and dynamic contrast-enhanced T1-weighted fat-suppressed sequences. Diffusion-weighted imaging was acquired using single-shot echo-planar imaging with b-values of 50 and 800 s/mm², and apparent diffusion coefficient maps were automatically generated on the workstation. Dynamic contrast-enhanced imaging was performed before and after intravenous administration of a gadolinium-based contrast agent (0.1 mmol/kg), followed by a saline flush.

Technical parameters were as follows: axial T1-weighted fast spin-echo (TR/TE, 484/8.5ms; slice thickness, 5 mm), axial and sagittal T2-weighted fat-suppressed fast spin-echo (TR/TE, 4786/82.5ms and 5116/83.5ms, respectively; slice thickness, 5 mm), and dynamic contrast-enhanced axial T1-weighted fat-suppressed sequence (TR/TE, 6.1/1.7ms; slice thickness, 2.2 mm).

All measurements were performed simultaneously by two radiologists with over ten years of experience in breast radiology.

Image Analysis

Two breast radiologists with over 10 years of experience in breast imaging independently reviewed all MRI examinations. The readers were blinded to the pathological results and to each other's assessments. Architectural distortion identified on FFDM was used as a reference to ensure accurate lesion correlation on MRI. Lesions were evaluated according to the American College of Radiology BI-RADS MRI descriptors, including lesion type, margin characteristics, internal enhancement pattern, background parenchymal enhancement, diffusion restriction, kinetic curve type, and T2 signal intensity. Following the independent readings, discrepant assessments were resolved in a second session by consensus to establish the final dataset used for analysis.

Interobserver agreement was assessed to evaluate the reliability of MRI feature interpretation. Cohen's kappa statistics were calculated for categorical variables, including lesion type, margin characteristics, internal enhancement pattern, background parenchymal enhancement category, presence of diffusion restriction, kinetic curve type, and high T2 signal intensity. Apparent diffusion coefficient measurements were evaluated using the intraclass correlation coefficient to assess agreement between readers. For ADC measurements, a single region of interest (ROI) was manually placed on the ADC map for each lesion. The ROI was positioned over the solid component of the lesion, corresponding to the area showing the most prominent diffusion restriction on DWI. Necrotic, cystic, or hemorrhagic areas were carefully avoided during ROI placement to ensure accurate measurement.

Statistical Analysis

All statistical analyses were performed using SPSS software (version 31.0, IBM Corp., Armonk, NY, USA). Descriptive statistics were presented as mean ± standard deviation (SD) for continuous variables and as frequency and percentage for categorical variables.

Comparisons between categorical variables, including lesion type, margin characteristics, internal enhancement, background parenchymal enhancement (BPE), diffusion restriction, kinetic curve type, and T2 signal intensity, and their association with pathological outcomes (benign vs. malignant) were evaluated using the chi-square test or Fisher's exact test, as appropriate.

Continuous variables, specifically ADC values, were compared between benign and malignant lesions using the independent samples t-test. Results were expressed with mean differences and 95% confidence intervals (CI).

Interobserver agreement for categorical MRI descriptors was assessed using Cohen's kappa statistics, while agreement for ADC measurements was evaluated using the intraclass correlation coefficient with a two-way random-effects model and absolute agreement definition. Kappa values were interpreted as follows: values less than 0.20 indicated slight agreement, 0.21–0.40 fair agreement, 0.41–0.60 moderate agreement, 0.61–0.80 substantial agreement, and values greater than 0.80 indicated almost perfect agreement.

A p-value < 0.05 was considered statistically significant.

Results

A total of 62 patients (age range, 18-76 years; mean 50.47±8.75 years) were included in the study. Thirty-six lesions were confirmed by surgical pathology and/or percutaneous biopsy, while the remaining 26 benign lesions were verified through a minimum

follow-up period of two years, during which no evidence of malignancy was detected at the initially suspected sites. Histopathological diagnoses comprised 17 malignant lesions, including nine invasive ductal carcinomas, one ductal carcinoma in situ, four invasive lobular carcinomas, one mucinous carcinoma, one tubular carcinoma, and one micropapillary carcinoma. In addition, 19 benign lesions were identified, consisting of 10 cases of fibrocystic disease, one atypical ductal epithelial hyperplasia, three sclerosing adenoses, one case of benign breast tissue, one fibrosis, two radial scars, and one lobular carcinoma in situ. MRI pathology findings for the study participants are depicted in Figure 1. Examples of FFDM, MRI findings, and kinetic curve analysis for atypical ductal hyperplasia, tubular carcinoma, and radial scar are presented in Figures 2, 3, and 4, respectively.

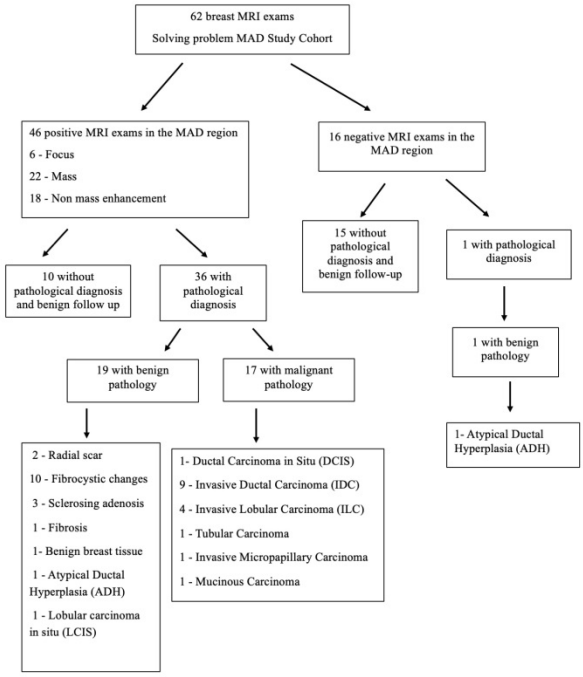

Fig. 1.
A flow chart illustrating the MRI findings across the patient cohort

Among the 17 patients with AD who were diagnosed with malignancy by biopsy, 14 were classified as luminal and 3 as non-luminal subtypes. Tumor grades were distributed as follows: 8 Grade 1, 7 Grade 2, and 2 Grade 3.

Architectural distortion without calcification was detected in 54 cases, of which 41 (75.9%) were benign and 13 (24.1%) malignant, whereas the presence of calcification was observed in 7 cases, including 3 (42.9%) benign and 4 (57.1%) malignant. The presence of calcification was associated with a higher malignancy rate; however, this association did not reach statistical significance (p=0.066) (Table I).

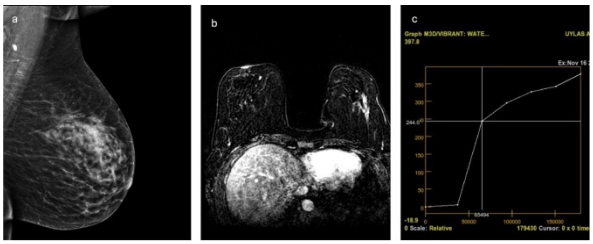

Fig. 2.
A 47-year-old female patient presented typical architectural distortion. Mammography mediolateral oblique (a) of the left breast shows architectural distortion in upper quadrant. Axial dynamic contrast-enhanced subtracted T1-weighted image (b) shows heterogenous enhancement of non-mass-like lesion with regional distribution. Enhancement kinetic curve (c) shows a medium rate persistent pattern. Pathologic result is atypical ductal hyperplasia

Table I. FFDM Findings

Category	Benign (n)	Malignant (n)	p-value
No Calcification	41 (75.9%)	13 (24.1%)	0.066 (Fisher 0.087)
With Calcification	3 (42.9%)	4 (57.1%)	
Breast Density A	1	1	0.733
Breast Density B	10	2	
Breast Density C	22	9	
Breast Density D	12	5	

FFDM, full field digital mammography

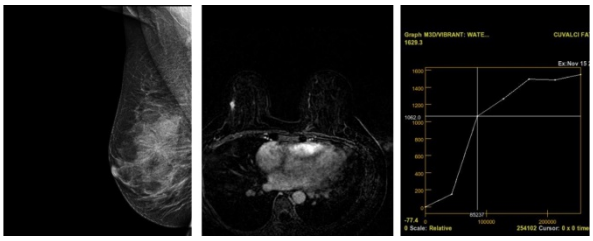

Fig. 3.
A 52-year-old female patient presented typical architectural distortion. Mammography mediolateral oblique (a) of the right breast shows architectural distortion in upper quadrant. Axial dynamic contrast-enhanced subtracted T1-weighted image (b) shows rim enhancement of round mass with not circumscribed margin. Enhancement kinetic curve (c) shows a medium rate plateau pattern. Pathologic result is invasive tubular carcinoma

Mammographic breast densities were classified for all patients and the relation in between the breast density and pathology results were evaluated. Breast density analysis showed no significant difference in benign versus malignant distribution across density categories A through D (p=0.733) (Table I).

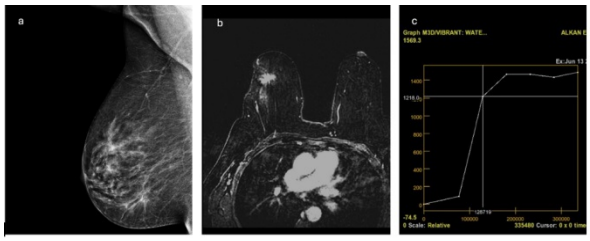

Fig. 4.
A 55-year-old female patient presented typical architectural distortion. Mammography mediolateral oblique (a) of the right breast shows architectural distortion in upper quadrant. Axial dynamic contrast-enhanced subtracted T1-weighted image (b) shows irregular mass with spiculated margin. Enhancement kinetic curve (c) shows a medium rate plateau pattern. Pathologic result is radial scar

Among the patients in whom background parenchymal enhancement (BPE) could be evaluated (n=46). In a subset of patients, BPE assessment was not feasible because of suboptimal image quality related to technical factors such as motion artifacts or inadequate fat suppression. Minimal BPE was associated with a higher malignancy rate (62.5%), while mild, moderate, and marked BPE were predominantly benign. This association reached statistical significance (p=0.026) (Table II).

Table II. MRI BPE and Lesion Type

Category	Benign (n)	Malignant (n)	p-value
Minimal BPE	6 (37.5%)	10 (62.5%)	0.026 (linear 0.003)
Mild BPE	12 (66.7%)	6 (33.3%)	
Moderate BPE	6 (85.7%)	1 (14.3%)	
Marked BPE	5 (100%)	0 (0.0%)	
Focus	3 (50.0%)	3 (50.0%)	
Mass	10 (45.5%)	12 (54.5%)	0.014 (linear 0.015)
NME	16 (88.9%)	2 (11.1%)	

MRI, magnetic resonance imaging
BPE, background parenchymal enhancement

Among the patients in whom lesion type could be evaluated on MRI (n=46), 22 had mass lesions, 18 demonstrated non-mass enhancement, and 6 presented with foci. Mass lesions were more frequently associated with malignancy (54.5%) compared with non-mass enhancements (11.1%), while foci were evenly distributed between benign and malignant outcomes. This relationship was statistically significant (p=0.014) (Table II).

Mass characteristics were also further evaluated. Among 22 cases with analyzable mass shape, irregular shape was more frequently malignant (69.2%) compared to oval or lobulated shape, but the difference did not reach significance (p=0.096). Margin assessment in 22 patients revealed that non-circumscribed margin was strongly associated with malignancy (78.6% vs. 12.5% in circumscribed), yielding a significant difference (p=0.003) (Table III). Internal enhancement patterns of 22 masses showed that homogeneous enhancement was mostly benign (66.7%), while all heterogeneous and rim-enhancing masses were malignant and this association was statistically significant (p=0.014) (Table III).

Among 18 cases of non-mass enhancement (NME), most focal, linear, and segmental distributions were benign, while malignancy was observed occasionally in regional distributions (Table). IV No significant association was identified between distribution pattern and pathology (p=0.852). In 18 NME cases where internal enhancement was assessable, homogeneous enhancement was exclusively benign, whereas heterogeneous patterns included two malignant cases; however, this difference was not statistically significant (p=0.156) (Table IV).

Table III. MRI Mass Morphology

Category	Benign (n)	Malignant (n)	p-value
Oval/Lobulated	6 (66.7%)	3 (33.3%)	0.096
Irregular	4 (30.8%)	9 (69.2%)	
Circumscribed Margin	7 (87.5%)	1 (12.5%)	0.003 (Fisher 0.006)
Non-circumscribed Margin	3 (21.4%)	11 (78.6%)	
Homogeneous Enhancement	10 (66.7%)	5 (33.3%)	0.014
Heterogeneous Enhancement	0	5 (100%)	
Rim Enhancement	0	2 (100%)	

MRI, magnetic resonance imaging

Table IV. MRI NME Findings

Category	Benign (n)	Malignant (n)	p-value
Focal	9 (90.0%)	1 (10.0%)	0.852
Linear/Ductal	2 (100%)	0	
Segmental	1 (100%)	0	
Regional	4 (80.0%)	1 (20.0%)	
Homogeneous Enhancement	8 (100%)	0	0.156
Heterogeneous Enhancement	8 (80%)	2 (20%)	

MRI, magnetic resonance imaging
NME, non-mass enhancement

Among the patients in whom T2 signal intensity could be assessed in 44 patients. T2 signal intensity assessment was not feasible in 2 patients, as the small lesion size precluded reliable evaluation despite detectable MRI findings. Among 28 lesions without high T2 signal, 14 (50.0%) were benign and 14 (50.0%) malignant, whereas among 16 lesions with high T2 signal, 13 (81.3%) were benign and 3 (18.8%) malignant. The difference was statistically significant, with absence of high T2 signal being associated with a higher malignancy rate (p=0.041).

Among the patients in whom kinetic curve analysis could be performed (n=43), persistent and plateau patterns were predominantly benign (85.7% and 69.2%, respectively), whereas wash-out curves were observed exclusively in malignant lesions (100%). This finding showed a highly significant association with pathology (p<0.001), and wash-out curves were strongly predictive of malignancy (Table V). Kinetic curve analysis could not be performed in 2 patients with non-mass enhancement and in 1 patient with a foci lesion.

Diffusion-weighted imaging findings were available in 37 patients. Diffusion restriction could not be assessed in 9 lesions due to small size and non-mass enhancement. Among 22 lesions without diffusion restriction, 21 (95.5%) were benign and only 1 (4.5%) malignant. In contrast, of the 15 lesions showing restricted diffusion, 4 (26.7%) were benign and 11 (73.3%) malignant. This difference was highly significant (p<0.001).

Table V. MRI High T2 Signal & Kinetic Curve

Category	Benign (n)	Malignant (n)	p-value
High T2 Absent	14 (50.0%)	14 (50.0%)	0.041
High T2 Present	13 (81.3%)	3 (18.8%)	
Persistent Curve	18 (85.7%)	3 (14.3%)	p<0.001
Plateau Curve	9 (69.2%)	4 (30.8%)	
Wash-out Curve	0	9 (100%)	

MRI, magnetic resonance imaging

The mean ADC value of benign lesions was significantly higher ($1.45\pm0.26\times10^{-3}$ mm²/s) compared with malignant lesions ($0.95\pm0.41\times10^{-3}$ mm²/s). Independent samples t-test demonstrated a highly significant difference between the two groups (p<0.001).

Among cases with NME, no statistically significant association was identified between distribution pattern or internal enhancement characteristics and pathological outcome. Given the limited number of NME cases, these findings should be interpreted cautiously and are presented as descriptive observations rather than definitive diagnostic indicators.

Discussion and Conclusion

In this retrospective study, we evaluated the diagnostic contribution of breast MRI in cases of AD detected on FFDM. Our findings demonstrated that lesion type, margin characteristics, internal enhancement patterns, diffusion restriction with ADC values, kinetic curve type, high T2 signal intensity, and BPE levels provided complementary information for differentiating benign from malignant lesions. In particular, diffusion restriction, lower ADC values, non-circumscribed margins, heterogeneous or rim enhancement, and wash-out kinetic patterns were more frequently observed in malignant lesions, whereas high T2 signal intensity and homogeneous enhancement were more commonly associated with benign outcomes.

The literature has consistently emphasized that AD represents a heterogeneous spectrum of abnormalities that may mimic benign entities. Gaur et al. reported substantial overlap between malignant and benign histopathological processes presenting as AD, highlighting the need for additional imaging modalities beyond mammography alone[4]. In line with these observations, our findings suggest that MRI, as an adjunct imaging technique, may aid in differentiating benign from malignant AD by providing combined morphologic descriptors (such as margin characteristics and enhancement patterns), functional information from diffusion-weighted imaging, and dynamic contrast-enhanced features.

The problem-solving role of MRI in the evaluation of AD has been demonstrated in several prior studies. Mei et al. showed that MRI provides incremental diagnostic value in mammographic AD categorized as BI-RADS 3–4[7], while Amitai et al. suggested that MRI may help exclude malignancy in selected AD cases[8]. Similarly, our results indicate that MRI, when interpreted using an integrated assessment of morphologic, functional, and kinetic features, contributes meaningful diagnostic information in distinguishing benign from malignant lesions in this challenging subgroup.

With respect to NME, statistical significance could not be demonstrated for subgroup analyses based on distribution patterns or internal enhancement characteristics. Although NMEs in our cohort were more frequently associated with benign outcomes, the limited number of NME cases and the absence of statistically significant differences preclude definitive conclusions. Therefore, these findings should be interpreted cautiously and should not be regarded as evidence of a causal relationship between specific NME features and benignity.

The heterogeneous nature of NME and the considerable overlap in imaging characteristics

between benign and malignant entities have been well documented in the literature. In this context, Aslan and Oktay demonstrated that the diagnostic accuracy of the Kaiser score—integrating lesion margins, kinetic enhancement patterns, internal enhancement, and the presence of edema—improves lesion characterization in cases of AD[6]. Consistent with their findings, our results suggest that combining morphologic and functional MRI features may enhance diagnostic confidence in AD; however, isolated NME descriptors alone appear insufficient for reliable differentiation, underscoring the importance of individualized assessment in this subgroup.

Our findings regarding BPE were also noteworthy. Minimal BPE was more frequently associated with malignancy, whereas marked BPE was observed only in benign cases. This observation supports previous reports suggesting that lower levels of BPE may improve lesion conspicuity and diagnostic performance, while higher BPE may obscure lesion characterization or be associated with benign hormonal effects[11]. It is also possible that minimal BPE reflects a relatively less hormonally stimulated parenchymal background, thereby increasing the contrast between malignant tissue and surrounding breast parenchyma. In addition, the predominance of malignancy among mass lesions compared with NMEs observed in our cohort is consistent with prior studies evaluating MRI features in mammographic AD[7].

From a functional imaging perspective, diffusion restriction and lower ADC values showed a strong association with malignancy. The diagnostic value of ADC in differentiating benign from malignant breast lesions has been confirmed in multiple prior studies[12,13], and our findings further support its role in the evaluation of AD. Kinetic curve analysis demonstrated that wash-out patterns were observed exclusively in malignant lesions, confirming the high specificity of this feature reported in earlier studies[14]. Conversely, high T2 signal intensity was more frequently associated with benignity, consistent with previous reports indicating that cystic or fibrous benign processes often exhibit high T2 signal intensity[15].

Invasive lobular carcinoma (ILC) was disproportionately represented among malignant lesions presenting as AD in our cohort. This finding is consistent with previous reports showing that ILC more commonly manifests as AD rather than as a discrete mass[16,17]. The characteristic single-file growth pattern of ILC, accompanied by stromal fibrosis and subtle distortion of ductolobular structures, provides a plausible histopathological explanation for this imaging presentation[18]. Furthermore, AD in our study was more frequently observed in low-grade and luminal-type breast cancers. Prior studies have similarly reported that luminal subtypes, particularly luminal A tumors, are more likely to present as AD, whereas high-grade or triple-negative tumors more often appear as well-defined masses[19,20].

Radial scar typically demonstrates a stellate fibroelastic core with entrapped ducts and lobules and frequently mimics invasive carcinoma on mammography[21]. Given the limited ability of MRI to reliably distinguish radial scar from malignancy in the setting of AD, a biopsy diagnosis of radial scar does not necessarily exclude coexistent carcinoma. Accordingly, management of these lesions should be guided by multidisciplinary evaluation. In our study, radial scar represented the most frequent source of diagnostic misclassification.

To our knowledge, this is one of the limited studies focusing specifically on BI-RADS 3–4 architectural distortion in a real-world problem-solving MRI cohort.

This study has several limitations. First, its single-center retrospective design and relatively small sample size limited statistical power in some subgroup analyses, particularly for NME. Second, a proportion of benign lesions was confirmed by imaging follow-up rather than histopathology, which may have introduced verification bias.

Breast MRI adds meaningful diagnostic value in the evaluation of AD detected on mammography. An integrated interpretation of morphologic, functional, and dynamic MRI features improves differentiation between benign and malignant lesions, particularly in BI-RADS 3–4 cases. This approach may help refine biopsy decisions and reduce unnecessary procedures, while recognizing the persistent overlap between benign sclerosing lesions and malignancy.

Researcher Contribution Statement:
Idea and design: S.G.; Data collection and processing: S.G., L.G.K.; Analysis and interpretation of data: S.G., L.G.K.; Writing of significant parts of the article: S.G.
Support and Acknowledgement Statement:
This research did not receive any specific grant from funding agencies in the public, commercial, or not-for-profit sectors.
Conflict of Interest Statement:
The authors declare that they have no conflict of interest.
Ethics Committee Approval Information:
Approving Committee: Ankara Bilkent Şehir Hastanesi 1 Nolu Tıbbi Araştırmalar Bilimsel ve Etik Kurulu
Approval Date: 13.08.2025
Decision No: 1/1607/2025

References

1. Zhang S, Shao Z, Yi H, et al. A comprehensive analysis of imaging features and clinical characteristics to differentiate malignant from non-malignant mammographic architectural distortion. Gland Surg 2024;13:669-683.
2. Choudhery S, Johnson MP, Larson NB, et al. Malignant Outcomes of Architectural Distortion on Tomosynthesis: A

Systematic Review and Meta-Analysis. AJR Am J Roentgenol 2021;217:295-303.

3. Shaheen R, Schimmelpenninck CA, Stoddart L, et al. Spectrum of diseases presenting as architectural distortion on mammography: multimodality radiologic imaging with pathologic correlation. Semin Ultrasound CT MR 2011;32:351-62.
4. Gaur S, Dialani V, Slanetz PJ, et al. Architectural distortion of the breast. AJR Am J Roentgenol 2013;201:W662-70.
5. Pautasso JJ, Van Speybroeck CDE, Michielsen K, et al. Comparative image quality and dosimetric performance of two generations of dedicated breast CT systems. Med Phys 2025;52:2191-2200.
6. Aslan O, Oktay A. Diagnostic accuracy of the breast MRI Kaiser score in suspected architectural distortions and its comparison with mammography. Sci Rep 2024;14:447.
7. Mei H, Xu J, Yao G, et al. The diagnostic value of MRI for architectural distortion categorized as BI-RADS category 3-4 by mammography. Gland Surg 2020;9:1008-1018.
8. Amitai Y, Scaranelo A, Menes TS, et al. Can breast MRI accurately exclude malignancy in mammographic architectural distortion? Eur Radiol 2020;30:2751-2760.
9. Pinker K, Moy L, Sutton EJ, et al. Diffusion-Weighted Imaging With Apparent Diffusion Coefficient Mapping for Breast Cancer Detection as a Stand-Alone Parameter: Comparison With Dynamic Contrast-Enhanced and Multiparametric Magnetic Resonance Imaging. Invest Radiol 2018;53:587-595.
10. Si L, Zhai R, Liu X, et al. MRI in the differential diagnosis of primary architectural distortion detected by mammography. Diagn Interv Radiol 2016;22:141-50.
11. Hu N, Zhao J, Li Y, et al. Breast cancer and background parenchymal enhancement at breast magnetic resonance imaging: a meta-analysis. BMC Med Imaging 2021;21:32.
12. Min Q, Kangwei S, Lu-lan Z, et al. Differential diagnosis of benign and malignant breast masses using diffusion-weighted magnetic resonance imaging. World Journal of Surgical Oncology 2015;13.
13. Tuan Linh L, Minh Duc N, Tra My TT, et al. Correlations between apparent diffusion coefficient values and histopathologic factors in breast cancer. Clin Ter 2021;172:218-224.
14. Kuhl CK, Schrading S, Bieling HB, et al. MRI for diagnosis of pure ductal carcinoma in situ: a prospective observational study. Lancet 2007;370:485-92.
15. Santamaría G, Velasco M, Bargalló X, et al. Radiologic and pathologic findings in breast tumors with high signal intensity on T2-weighted MR images. Radiographics 2010;30:533-48.
16. Johnson K, Sarma D, Hwang ES. Lobular breast cancer series: imaging. Breast Cancer Res 2015;17:94.
17. Bachert SE, Jen A, Denison C, et al. Breast lesions associated with mammographic architectural distortion: a study of 588 core needle biopsies. Mod Pathol 2022;35:728-738.
18. Lee JH, Park S, Park HS, et al. Clinicopathological features of infiltrating lobular carcinomas comparing with infiltrating ductal carcinomas: a case control study. World J Surg Oncol 2010;8:34.
19. Liu H, Zhan H, Sun D, et al. Comparison of BSGI, MRI, mammography, and ultrasound for the diagnosis of breast lesions and their correlations with specific molecular subtypes in Chinese women. BMC Med Imaging 2020;20:98.
20. Lopez JK, Bassett LW. Invasive lobular carcinoma of the breast: spectrum of mammographic, US, and MR imaging findings. *Radiographics* 2009;29:165–176.
21. Rakha E, Beca F, D'Andrea M, et al. Outcome of radial scar/complex sclerosing lesion associated with epithelial proliferations with atypia diagnosed on breast core biopsy: results from a multicentric UK-based study. J Clin Pathol 2019;72:800-804.